Strathprints Institutional Repository

Enhanced frequency up-conversion in Rb vapor

A. Vernier,[1] S. Franke-Arnold,[1] E. Riis,[2] and A. S. Arnold[2,*]

[1]*SUPA, Dept. of Physics and Astronomy, University of Glasgow, Glasgow G12 8QQ, UK*
[2]*SUPA, Dept. of Physics, University of Strathclyde, Glasgow G4 0NG, UK*
**a.arnold@phys.strath.ac.uk*

Abstract: We demonstrate highly efficient generation of coherent 420 nm light via up-conversion of near-infrared lasers in a hot rubidium vapor cell. By optimizing pump polarizations and frequencies we achieve a single-pass conversion efficiency of 260% per Watt, significantly higher than in previous experiments. A full exploration of the coherent light generation and fluorescence as a function of both pump frequencies reveals that coherent blue light is generated close to ^{85}Rb two-photon resonances, as predicted by theory, but at high vapor pressure is suppressed in spectral regions that do not support phase matching or exhibit single-photon Kerr refraction. Favorable scaling of our current 1 mW blue beam power with additional pump power is predicted.

OCIS codes: (190.4380) Nonlinear optics, four-wave mixing; (270.1670) Coherent optical effects.

References and links

1. F. Nez, F. Biraben, R. Felder and Y. Millerioux, "Optical frequency determination of the hyperfine components of the $5S_{1/2}$-$5D_{3/2}$ two-photon transitions in rubidium," Opt. Commun. **102**, 432–438 (1993).
2. M. J. Snadden, A. S. Bell, E. Riis and A. I. Ferguson, "Two-photon spectroscopy of laser-cooled Rb using a mode-locked laser," Opt. Commun. **125**, 70–76 (1996).
3. A. J. Olson, E. J. Carlson and S. K. Mayer, "Two-photon spectroscopy of rubidium using a grating-feedback diode laser," Am. J. Phys. **74**, 218–223 (2006).
4. M. Xiao, Y. Q. Li, S. Z. Jin and J. Gea-Banacloche, "Measurement of dispersive properties of electromagnetically induced transparency in rubidium atoms," Phys. Rev. Lett. **74**, 666–669 (1995).
5. S. D. Badger, I. G. Hughes and C. S. Adams, "Hyperfine effects in electromagnetically induced transparency," J. Phys. B **34**, L749–L756 (2000).
6. A. S. Arnold, J. S. Wilson and M. G. Boshier, "A simple extended-cavity diode laser," Rev. Sci. Instrum. **69**, 1236–1239 (1998).
7. M. S. Malcuit, D. J. Gauthier and R. W. Boyd, "Suppression of amplified spontaneous emission by the four-wave mixing process," Phys. Rev. Lett. **55**, 1086–1089 (1985).
8. S. M. Hamadani, J. A. D. Stockdale, R. N. Compton and M. S. Pindzola, "Two-photon resonant four-wave mixing and multiphoton ionization of cesium in a heat-pipe oven," Phys. Rev. A **34**, 1938–1943 (1986).
9. D. V. Sheludko, Simon C. Bell, R. Anderson, C. S. Hofmann, E. J. D. Vredenbregt, and R. E. Scholten, "State-selective imaging of cold atoms," Phys. Rev. A **77**, 033401 (2008).
10. H. Ohadi, M. Himsworth, A. Xuereb, and T. Freegarde, "Magneto-optical trapping and background-free imaging for atoms near nanostructured surfaces," Opt. Express **17**, 23003–23009 (2009).
11. A. I. Lvovsky, S. R. Hartmann and F. Moshary, "Omnidirectional superfluorescence," Phys. Rev. Lett. **82**, 4420–4423 (1999).
12. A. S. Zibrov, M. D. Lukin, L. Hollberg and M. O. Scully, "Efficient frequency up-conversion in resonant coherent media," Phys. Rev. A **65**, 051801 (2002).
13. T. Meijer, J. D. White, B. Smeets, M. Jeppesen, and R. E. Scholten, "Blue five-level frequency-upconversion system in rubidium," Opt. Lett. **31**, 1002–1004 (2006).

#128183 - $15.00 USD Received 10 May 2010; revised 11 Jun 2010; accepted 19 Jul 2010; published 27 Jul 2010

14. A. M. Akulshin, R. J. McLean, A. I. Sidorov, and P. Hannaford, "Coherent and collimated blue light generated by four-wave mixing in Rb vapour," Opt. Express **17**, 22861–22870 (2009).
15. Kurucz data, cfa-www.harvard.edu/amp/tools.html.
16. P. Siddons, C. S. Adams, C. Ge and I. G. Hughes, "Absolute absorption on rubidium D lines: comparison between theory and experiment," J. Phys. B **41**, 155004 (2008).
17. J. L. Hall, M. Zhu and P. Buch, "Prospects for using laser-prepared atomic fountains for optical frequency standards applications," J. Opt. Soc. Am. B **6**, 2194–2205 (1989).
18. G. Morigi, S. Franke-Arnold, and G.-L. Oppo, "Phase-dependent interaction in a four-level atomic configuration," Phys. Rev. A **66**, 053409 (2002).
19. S. Kajari-Schröder, G. Morigi, S. Franke-Arnold, and G.-L. Oppo, "Phase-dependent light propagation in atomic vapors," Phys. Rev. A **75**, 013816 (2007).
20. J. T. Schultz, S. Abend, D. Döring, J. E. Debs, P. A. Altin, J. D. White, N. P. Robins and J. D. Close, "Coherent 455nm beam production in cesium vapor," Opt. Lett. **34** 2321–2323 (2009).

Nonlinear optical processes can be greatly enhanced for quasi-resonant atomic and molecular systems, allowing phenomena like efficient frequency up-conversion, four-wave mixing, slow light or image storage to be studied at low light intensities. On resonance, absorption hinders the build-up of strong coherences; this can be counteracted by excitation via two-photon resonances and in particular by using electromagnetically induced transparency (EIT). Here we report the generation of 1.1 mW of 420 nm blue light by enhanced frequency up-conversion in a hot rubidium vapor. This is made possible by long lived two-photon coherences at frequencies that allow propagation under phase-matching conditions. Depending on the polarization of the pump lasers, up-conversion can be enhanced or almost completely suppressed.

Alkali metal vapors are versatile tools for spectroscopy and nonlinear optics in atomic physics and have long been used for studies of 2-photon spectroscopy [1, 2, 3], dispersion [4] and EIT [4, 5]. In both isotopes of rubidium, the $5S_{1/2} - 5P_{3/2}$ (780 nm) and $5P_{3/2} - 5D_{5/2}$ (776 nm) transitions (Fig. 1a) are easily accessible with simple diode laser systems [6]. The extremely strong dipole moment of the infrared $6P_{3/2} - 5D_{5/2}$ transition (Fig. 1b) means that two-photon pumping with 776 and 780 nm light facilitates three-photon coherence between ground state and the $6P_{3/2}$ level. Excitation and decay via other levels ($5P_{1/2}$, $6P_{1/2}$, $5D_{3/2}$) is excluded by large detuning and selection rules. Similar alkali metal transitions have proven ideal for studies of amplified spontaneous emission versus four-wave mixing [7, 8], superfluorescence [11], multi-photon ionization processes [8], and sensitive atomic imaging [9, 10].

Recent papers [12, 13, 14] have reported the generation of tens of μWatts of coherent 420 nm blue light by pumping the Rb 5S−5P−5D transition. In our experiment we obtained

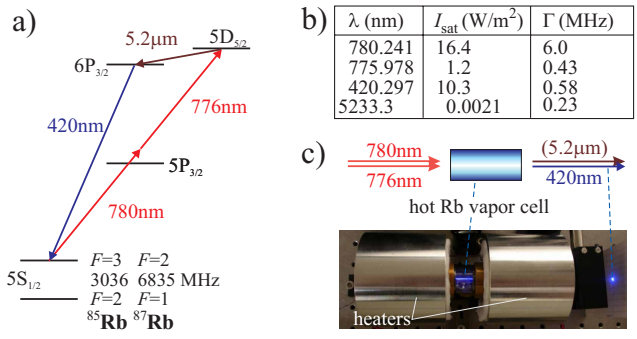

Fig. 1. a) The Rb energy level scheme. b) Relevant Rb transition parameters [15]. c) Experimental image showing how co-propagating focussed 780 and 776 nm laser beams create a coherent 420 nm (and invisible 5.2 μm) beam.

#128183 - $15.00 USD Received 10 May 2010; revised 11 Jun 2010; accepted 19 Jul 2010; published 27 Jul 2010

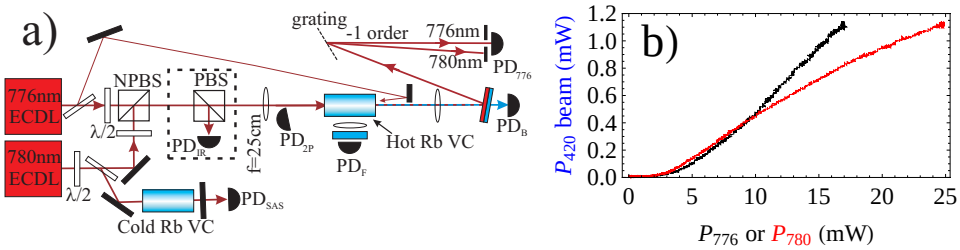

Fig. 2. a) Experimental schematic, abbreviations used are: PD (photodiode), VC (vapor cell) N/PBS (non/polarizing beamsplitter) and ECDL (external cavity diode laser). b) Power in the coherent 420 nm beam as a function of 780 nm (red) and 776 nm (black) input power. For each trace the power of the other input beam was maximal and detunings and polarization were optimized, see text.

up to 1.1 mW of coherent blue light for similar input pump powers. We have studied and optimized blue light generation for a variety of experimental parameters, namely input beam polarization and frequency, and Rb vapor pressure. In our system we have measured a maximum of 1.1 mW of coherent blue light close to two-photon resonance of the input lasers at $\Delta_{780} = -\Delta_{776} \cong 1.6$ GHz. Optimal conditions include a Rb vapor pressure of 10^{-3} mbar and co-circularly polarized input beams at maximum available powers of 17 mW at 776 nm and 25 mW at 780 nm. This corresponds to a conversion efficiency of $\eta = P_{420}/(P_{776}P_{780}) \sim 260\%/\mathrm{W}$.

The essence of the experimental setup is shown in Fig. 1c), with a more detailed view in Fig. 2a). Laser beams from Faraday-isolated 776 nm and 780 nm extended-cavity diode lasers are overlapped on a non-polarizing beamsplitter and focussed into a 75 mm long Rb vapor cell. The pump beams have maximum powers of 17 mW and 25 mW respectively which for elliptical beams with waists of 0.6 mm $\times$ 1.1 mm yield an estimated focal intensity of $\approx 2 \times 10^6\,\mathrm{W/m^2}$ each. Note that the 780 nm beam area after the cell varies with frequency, differing by more than an order of magnitude due to Kerr lensing.

We have measured the conversion efficiency as a function of the 776 and 780 nm input power (Fig. 2b), with all other parameters fixed at their optimum values stated above. We note that conversion efficiency depends on the Rabi frequencies and detunings of the pump beams, so that for low pump powers the chosen detunings are not ideal. The pump power was varied by rotating half wave plates in the individual input beams, and monitored via the polarizing beamsplitter (PBS) shown in the dashed region of Fig. 2a). Although the blue light begins to saturate with 780 nm input power, it is linear in 776 nm input power in the regions accessible by our diode lasers, promising a further increase in blue light power for stronger 776 nm pumping.

The atomic density and associated vapor temperature were measured to high resolution via absorption spectroscopy of a low power (5 μW) 780 nm probe beam [16]. This avoided any inaccuracy due to the inhomogeneity of the external cell temperature. For our setup optimal blue light generation occurs at a temperature of $120 \pm 1^\circ$C, corresponding to a Rb vapor pressure of 9×10^{-4} mbar, nearly 4 orders of magnitude higher than at room temperature. While higher temperatures, and therefore atomic densities, facilitate the nonlinear up-conversion process, they also increase absorption of the pump and output beams. Overall, the system is fairly robust: more than half of the maximum blue beam efficiency could be achieved over a temperature range of $104 - 131^\circ$C corresponding to a factor of 5 in Rb pressure, and focussing the near-infrared light from 0.4 to 4 times the optimal free-space focal intensity yielded similar ($> 75\%$ of optimal) conversion efficiency.

In order to investigate the up-conversion process we have measured fluorescent and coherent blue light generation over a wide range of input beam frequencies, see Fig. 3c)-f). Data was

#128183 - $15.00 USD Received 10 May 2010; revised 11 Jun 2010; accepted 19 Jul 2010; published 27 Jul 2010

taken for low and high Rb temperatures of 90°C and 120°C respectively, corresponding to vapor pressures of 1×10^{-4} mbar and 9×10^{-4} mbar. The frequency of the 780 nm beam was measured via saturated absorption spectroscopy in a room temperature Rb cell, and that of the 776 nm beam by monitoring the two-photon absorption of a weak 776 nm probe beam counter-propagating through the hot cell (Fig. 2a).

We have modeled fluorescence and coherent light generation (Fig. 3a) and b) from optical Bloch equations for the 5 atomic levels, using a similar model to Ref. [13], evaluated with Doppler broadening (FWHM$\sim$ 580 MHz for the 776 and 780 nm light at $\sim$ 100°C) and for Rabi frequencies ($\Omega_{780} = 1.4$ GHz, $\Omega_{776} = 0.4$ GHz, $\Omega_{IR} = 30$ MHz, $\Omega_{420} = 20$ MHz) similar to the estimated experimental focal values in the low pressure cell. The model does not explicitly include propagation, and neglects the hyperfine structure of the upper states. Nevertheless, numerical solutions for the steady state of the optical Bloch equations allowed us to interpret many of the observed features. Fluorescence (top row of Fig. 3) arises from a transfer of population to the 5D level and subsequent fast decay to the 6P level. Our model shows that this happens mainly when the system is pumped at two-photon resonance between the Stark-shifted atomic levels, and to a lesser extent, for resonant driving of the 776 nm transition. The model (Fig. 3a) describes the observed fluorescence well (Figs. 3c and e), even though it does not account for propagation effects or 780 nm pump Kerr lensing which increase at higher temperature.

The generation of coherent blue light requires coherences between the ground state 5S hy-

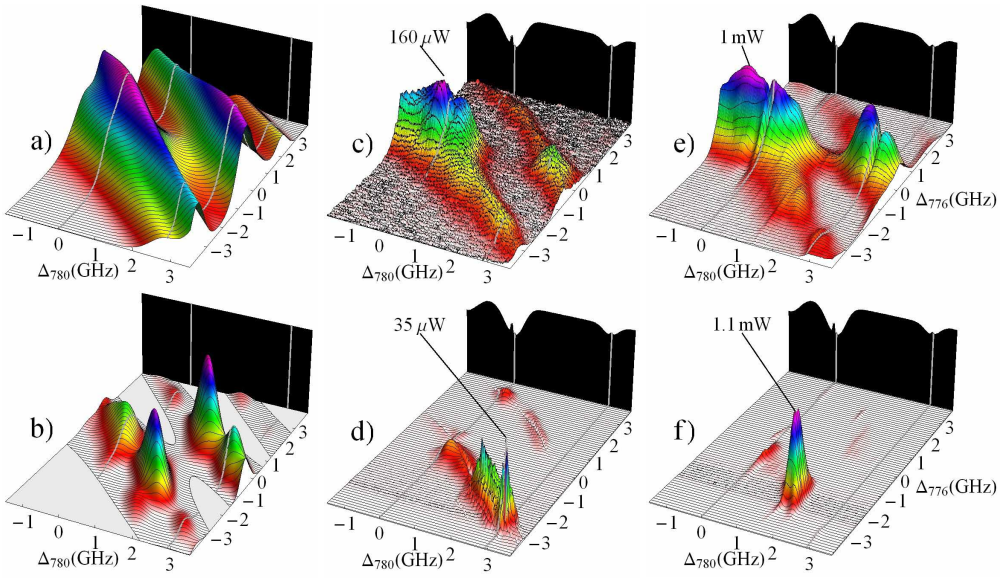

Fig. 3. Relative blue fluorescence (top row) and blue beam (bottom row) power as a function of 780 and 776 nm light detuning. Theoretical simulations of the 5-level Bloch equations are shown in a) and b). Graph a) shows the Doppler-broadened population in the 6P level corresponding to blue fluorescence. Fig. b) shows the Doppler-broadened coherences between ground and the 6P level, corresponding to coherent blue light generation. The blue coherences are adjusted to account for Kerr lensing and absorption of the 780 nm pump beam. Graphs c) and d) show measurements at a cell temperature of 90°C, and e) and f) at 120°C. At low pressure, coherent light is generated over a range of detunings at two-photon resonance. At high pressure Kerr-lensing of the pump beams and phase-matching become more pronounced, restricting blue light generation to a narrow frequency window. The backdrops show 780 nm saturated absorption in a cold cell.

#128183 - $15.00 USD Received 10 May 2010; revised 11 Jun 2010; accepted 19 Jul 2010; published 27 Jul 2010

perfine levels and the 6P level. While the detuning of the blue (and IR) light is experimentally unknown, our simulations suggest that coherent blue light conversion occurs at three-photon resonance. For the (relatively) small blue light and IR intensities in the experiment the 6P level is unshifted, so three-photon resonance coincides with two-photon resonance. Phase-matching is a prerequisite of efficient coherent light generation. Our model shows that phase-matching $\Delta k = n_{780}k_{780} + n_{776}k_{776} - n_{IR}k_{IR} - n_{420}k_{420} \approx 0$ is satisfied along most of the three-photon resonances. We model blue light generation (Fig. 3b) as Doppler-broadened coherences adjusted to account for Kerr lensing and absorption of the 780 nm pump beam. This is an approximation to a full analysis which would require the study of field and density matrix propagation for non-collinear beams. At lower vapor pressure, we observe coherent blue light over a range of detunings near two-photon resonance (Fig. 3d), reminiscent of observations in Ref. [13, 14]. Strikingly, when the Rb pressure in the cell is high, the experiment shows an increase of blue beam generation by 1.5 orders of magnitude, however only over a restricted range of input detunings (Fig. 3f), with highest conversion efficiency for two-photon (and three-photon) resonance at $\Delta_{780} = -\Delta_{776} = 1.6$ GHz. We attribute the suppression of blue light generation outside this region to Kerr-lensing of the 780 nm input beam. Furthermore, absorption of 780 nm light contributes to the absence of light generation from the ^{87}Rb isotope.

A scan (Fig. 4) of the 780 nm input frequency, keeping the 776 nm detuning constant at the optimized value of $\Delta_{776} = -1.6$ GHz, shows clearly the strong frequency dependence of fluorescence and blue light generation. The theoretical model (Fig. 4a) of blue fluorescence accompanied by 776 nm absorption agrees well with the experiment (Fig. 4c). Coherences on the 420 nm transition between the 5S level and 6P level are present at two-photon resonance for the two hyperfine ground levels of ^{85}Rb and ^{87}Rb, and mark out four frequency regions of potential blue light generation, Fig. 4b). Kerr-lensing depletes and deflects the 780 nm pump laser at three of these resonances, so that only the coherence at $\Delta_{780} = 1.6$ GHz survives. The same

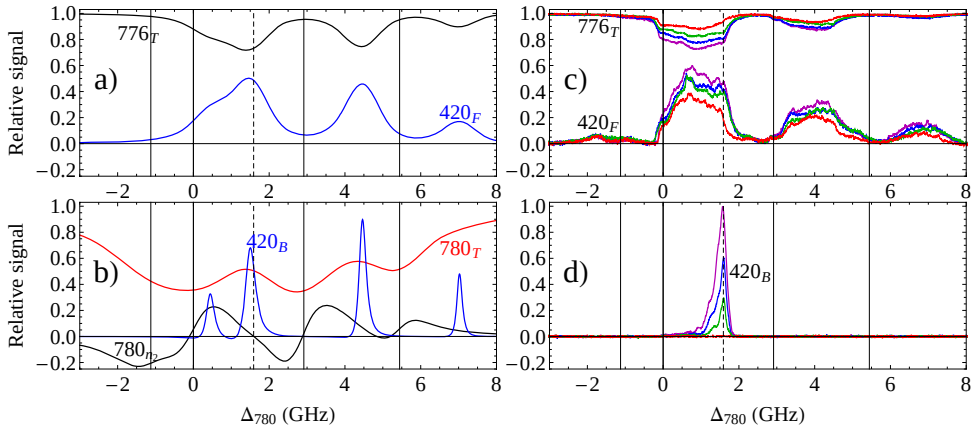

Fig. 4. Coherent and fluorescent blue light as a function of Δ_{780} for $\Delta_{776} = -1.6$ GHz. Graph a) shows theoretical blue fluorescence (420_{F}, blue) as well as transmission of the 776 nm (776_{T}, black) pump beam, including Doppler-broadening. Graph b) shows the blue beam coherences (420_{B}, blue), as well as the Doppler-broadened theoretical transmission (780_{T}, red) and Kerr-lensing ($780_{n_2} \propto \Delta n_{780}/\Delta I_{780}$ intensity-dependent refraction, black) of the 780 nm beam, which favors the coherence at 1.6 GHz. Measurements of blue fluorescence accompanied by 776 nm absorption c), and blue beam generation d) are shown for different input polarizations: counter-circular (red), crossed-linear (green), co-linear (blue) and co-circular (purple). Vertical lines indicate ^{85}Rb and ^{87}Rb 780 nm resonances.

#128183 - $15.00 USD Received 10 May 2010; revised 11 Jun 2010; accepted 19 Jul 2010; published 27 Jul 2010

detuning also exhibits a local minimum of absorption of the 780 nm input laser. We note that Kerr lensing will change beam direction and hence also modify the phase-matching condition. Increasing the atomic density and hence the optical path length, makes propagation effects and phase-matching more critical and adds further complexity as more 5 μm and 420 nm fields are generated. Experimentally, the strongest blue light generation was observed near a minimum of lensing for the 780 nm beam, Fig. 4d).

We finally report the crucial effect of input polarization on blue light generation, shown in Fig. 4c) and d). For these experiments the PBS in the dashed region of Fig. 2a) had to be removed. We simultaneously monitored the blue beam power (PD_B), the blue fluorescence in the cell (PD_F), absorption of the 776 nm beam (PD_{776}), and the detuning of the 780 nm laser (PD_{SAS}). Measurements were taken for four different relative input polarizations of the 776 nm and 780 nm input beams: co-linear, crossed-linear, co-circular and counter-circular. Care was taken to compensate for grating polarization-dependence in the 776 nm pump beam measured at PD_{776}. By analyzing the 776 nm laser absorption (Fig. 4c), we can estimate that it is possible to create a coherent 420 nm photon for every six 776 nm photons absorbed. Note that the blue beam generation is suppressed by a factor of 500 when counter-circular polarization is used, although there is still a similar amount of blue fluorescence and 776 nm beam absorption, indicating that the transfer of population to levels $5D_{5/2}$ and $6P_{3/2}$ is not forbidden by two- and three-photon absorption selection rules. This implies that the excitation of three-photon coherences between the $5S_{1/2}$ ground state and the $6P_{3/2}$ state depend crucially on polarization. Optical pumping favors blue light generation for the case of co-circularly polarized pump beams, however, the inhibition of blue light generation for counter-circular polarization suggests an interference effect. This may be attributed to a cancelation of the coherences due to the phase of the atomic dipoles. One can envisage that this property will be useful for applications in optical switching, where flipping 780 nm (or 776 nm)pump polarization would switch the blue beam power.

As our system is not saturating with pump power, increasing the pump power or using a build-up cavity could generate tens of mW of blue light. By accessing higher lying $D_{5/2}$ levels one should be able to generate similar powers at UV wavelengths by transitions via the corresponding $P_{3/2}$ levels. It is interesting to consider the application of such light sources for laser cooling where the narrower linewidth on these blue/UV transitions will lead to much lower Doppler temperatures [17]. In initial experiments we have observed 420 nm linewidths of less than 8 MHz, at the resolution limit of our etalon. The scheme should generalize to all alkali metals, and has recently been realized in cesium [20].

In conclusion, we have observed a polarization-dependent factor of 26 increase in blue light conversion efficiency under comparable conditions to previous experiments. Our observations of the frequency-dependent characteristics of the 776 nm beam absorption, blue fluorescence and blue beam power show good agreement with our theoretical framework, particularly for low experimental temperatures, indicating the importance of three-photon resonance coinciding with vanishing susceptibility on the 780 nm transition. In the low Rb pressure regime with the weaker blue beam afforded by crossed-linear polarizations we observe similar experimental behavior (frequency dependence and conversion efficiency) as observed in Refs. [12, 13] and we attribute our increased efficiency to polarization enhancement as well as a higher apparent Rb vapor pressure. It is clear that propagation must be included for proper modeling of the system at high temperatures due to the strong absorption/refraction processes at work in the cell. There are still many open questions in this surprisingly rich atomic vapor system. We envisage future experiments in isotopically enhanced vapor cells (to simplify the system's absorption-emission characteristics) and sapphire vapor cells which will allow us access to the 'missing link' of the closed loop structure [18, 19], the 5.2 μm light.

#128183 - $15.00 USD Received 10 May 2010; revised 11 Jun 2010; accepted 19 Jul 2010; published 27 Jul 2010

Acknowledgements

Thanks to N. Paterson, S. Clark and N. Houston for experimental contributions. We gratefully acknowledge discussions with P. Siddons and I. G. Hughes. SFA is a RCUK Research Fellow.

#128183 - $15.00 USD Received 10 May 2010; revised 11 Jun 2010; accepted 19 Jul 2010; published 27 Jul 2010